Flow Versus Uptake Comparisons of Thallium-201 with Technetium-99m Perfusion Tracers in a Canine Model of Myocardial Ischemia

Michael J. Meleca, Anthony J. McGoron, Myron C. Gerson, Ronald W. Millard, Marjorie Gabel, Danuta Biniakiewicz, Nancy J. Roszell and Richard A. Walsh

Division of Cardiology, Department of Internal Medicine; E. L. Saenger Radioisotope Laboratory; Division of Nuclear Medicine, Department of Radiology; and Department of Pharmacology and Cell Biophysics, University of Cincinnati College of Medicine, Cincinnati, Ohio

We investigated the myocardial flow kinetics of six putative radioperfusion agents (^{99m}Tc-Q3, ^{99m}Tc-Q4, ^{99m}Tc-Q12, ^{99m}Tc-sestamibi, ^{99m}Tc-tetrofosmin and ^{99m}TcN-NOET) and ^{201}Tl in a canine model of myocardial ischemia with pharmacologic coronary artery vasodilation. **Methods:** In 31 open-chest dogs with acute coronary occlusion, dipyridamole (~0.56 mg/kg) was infused intravenously, followed by a perfusion tracer injection and radioactive microspheres for myocardial blood flow (MBF) measurement. The paired data were normalized using three techniques; average, normal or maximum myocardial tracer activity and MBF. **Results:** The upper limit of MBF obtained for the group of tracers ranged from 4.2 ml/min/g to 8.2 ml/min/g. There was a statistically significant ($p < 0.0001$) linear correlation ($r = 0.87$–0.98) between the normalized myocardial activity and the normalized MBF values of each of the tracers. The slope of the curve normalized by average for ^{201}Tl (0.83) was greater than those for the ^{99m}Tc tracers, and the intercept (0.07) was lower than those for the ^{99m}Tc tracers. Slopes and intercepts for the ^{99m}Tc agents were as follows: ^{99m}Tc-Q3, 0.81 and 0.18; ^{99m}Tc-Q4, 0.61 and 0.41; ^{99m}Tc-Q12, 0.63 and 0.39; ^{99m}Tc-sestamibi, 0.62 and 0.34; ^{99m}Tc-tetrofosmin, 0.68 and 0.32; and ^{99m}TcN-NOET, 0.71 and 0.29, respectively. **Conclusion:** In an anesthetized open-chest canine model of regional myocardial ischemia with dipyridamole induced hyperemia, ^{201}Tl shows a more ideal relationship between tracer uptake and MBF than do the ^{99m}Tc-based agents. Of the various ^{99m}Tc-based imaging agents studied, the myocardial flow kinetics of ^{99m}Tc-Q3 appear to be closest to ideal. This relationship is maintained regardless of the normalization technique used. This may, in theory, imply a higher sensitivity in discerning ischemic from normal myocardium and a role in diagnostic nuclear imaging for ^{99m}Tc-Q3.

Key Words: myocardium; ischemia; perfusion imaging; microspheres; technetium-99m

J Nucl Med 1997; 38:1847–1856

The noninvasive assessment of coronary artery disease by nuclear tracer imaging is based on the principle that the myocardial extraction of the radioperfusion agent is related to myocardial blood flow (MBF) over a wide range of flows. An ideal perfusion tracer would display a linear flow relationship with a slope equal to 1.0 and a 0.0 y-intercept. A tracer displaying a lower slope or a positive y-intercept would, in theory, be less sensitive in discriminating normal from ischemic myocardium. When pharmacologic agents are used to increase coronary blood flow (as much as 4–5 times baseline normal levels) (*1–4*), a linear tracer-to-MBF relationship would enhance image contrast between high- and low-flow areas. Although several studies have addressed the uptake of individual radiotracers in animal models (*5–20*), wide variations in experimental technique and statistical methods make tracer comparisons difficult.

Here, we report a study in which we investigated the relationship of myocardial extraction to MBF for seven perfusion agents (^{201}Tl, ^{99m}Tc-Q3, ^{99m}Tc-Q4, ^{99m}Tc-Q12, ^{99m}Tc-sestamibi, ^{99m}Tc-tetrofosmin and ^{99m}TcN-NOET) in a canine model of coronary artery occlusion with dipyridamole-induced coronary hyperemia. We used three normalization techniques to allow a comparison of our data to those previously published by us (*6*) and to compare the effects of different normalization methods (*7,8,21*) on data analysis. In addition, we describe the uptake kinetics and the chemical nature of the new mixed ligand Q compound, ^{99m}Tc-Q4.

MATERIALS AND METHODS

Animal Instrumentation

Animal studies conformed to the guidelines of the American Physiologic Society and were approved by the Institutional Animal Care and Use Committee. Thirty-six male mongrel dogs weighing 19.0 kg–30.0 kg were instrumented. Four dogs developed sustained ventricular fibrillation after coronary artery occlusion and required prolonged resuscitation and support with inotropic drugs. These animals were excluded from all further consideration. Eight dogs, randomly distributed among the tracer groups, developed ventricular fibrillation and were resuscitated with electrical cardioversion. Sinus rhythm was subsequently restored along with hemodynamic stability before tracer administration. A total of 32 dogs were studied to compare initial myocardial tracer distribution to MBF, as assessed by radiolabeled microspheres for seven radioperfusion agents [^{201}Tl ($n = 5$), ^{99m}Tc-Q3 ($n = 9$), ^{99m}Tc-Q4 ($n = 4$), ^{99m}Tc-Q12 ($n = 7$), ^{99m}Tc-sestamibi ($n = 4$), ^{99m}Tc-tetrofosmin ($n = 4$) and ^{99m}TcN-NOET ($n = 4$)]. The five animals injected with ^{201}Tl also received a ^{99m}Tc tracer.

The animals were sedated with morphine sulfate (3 mg/kg) subcutaneously and were anesthetized with pentobarbital (20 mg/kg) intravenously. These drugs were supplemented as needed. The animals were intubated with a cuffed endotracheal tube, placed on a positive-pressure ventilator and ventilated with room air, supplemented with 95% O_2 and 5% CO_2, to maintain an arterial blood pO_2 of >100 mmHg. The thorax was entered through a left lateral thoracotomy at the fourth intercostal space, and the heart was suspended in a pericardial cradle. A ligature was placed on the left anterior descending artery (LAD), distal to the first major diagonal branch, or on the left circumflex artery (LCX), 3 cm–4 cm from its origin.

A catheter was placed in the left atrium to allow pressure recording and radiolabeled microsphere injection. Another catheter

Received Sep. 4, 1996; revision accepted Feb. 3, 1997.

For correspondence or reprints contact: Anthony J. McGoron, PhD, E. L. Saenger Radioisotope Laboratory, Division of Nuclear Medicine, Department of Radiology, University of Cincinnati, P.O. Box 670577, Cincinnati, OH 45267-0577.

was inserted through a femoral artery and advanced into the ascending aorta for measurement of central aortic pressure. A separate arterial catheter for the withdrawal of reference microsphere blood was advanced into the central aorta. A femoral vein was cannulated for administration of intravenous fluids and a continuous lidocaine infusion at 1 mg/min–2 mg/min. Additional lidocaine was administered intravenously and topically to the heart, as needed, for treatment of arrhythmias. A separate femoral vein catheter for the administration of dipyridamole and the chosen radiopharmaceutical was advanced until its tip lay near the right atrium. A thermal pad was placed under the animal to assure normothermia during the study. Specimens of arterial blood were obtained at frequent intervals to assess pH, pO_2 and pCO_2. Appropriate adjustments were made as required to keep these parameters within the physiologic range.

Radiopharmaceuticals

Thallium-201 was obtained commercially from DuPont/NEN Medical Products (Boston, MA). Technetium-99m-Q3 was prepared as previously described (*5*). Technetium-99m-Q12 (furifosmin) was prepared from kits as previously described (*22*). Technetium-99m-sestamibi (Cardiolite) was prepared from kits provided by DuPont/NEN Medical Products. Technetium-99m-tetrofosmin was prepared from kits provided by Amersham International. Technetium-99m-N-NOET was prepared from kits provided by CIS Bio International (Gif-sur-Yvette, France).

The synthesis of ^{99m}Tc-Q4 has not been previously reported. We synthesized the Schiff base ligand, 3-ethoxycarbonyl-9-methyl-5,8-diazadodeca-3,9-diene-2,11-dione, after a modification of the general reaction sequence described earlier (*23*). Freshly distilled pentane-2,4-dione (0.02 mol in 40 ml of chloroform) was added dropwise to a stirred and cooled solution of 1,2-diaminoethane (0.06 mol in 60 ml of chloroform). After addition was complete, the mixture was stirred for an additional 4 hr at a temperature not exceeding 10°C. Then, the chloroform was distilled off under an efficient water aspirator, and the excess of diamine was distilled off quickly under a 0.05-mmHg vacuum. The yellow, oily residue after distillation was redissolved in 50 ml of absolute ethanol, and to this solution, 2-ethoxymethylene-3-oxobutanoate (0.018 mol), obtained by the method of Claisen (*24*), was added at once. The reaction mixture was stirred at room temperature (~25°C) for 1 hr, followed by addition of 50 ml of hexane and overnight refrigeration at 4°C. The precipitate formed was filtered off. The filtrate was evaporated to dryness, and the crystalline residue was recrystallized several times from mixtures of ethylene chloride and hexane or isopropyl alcohol and diisopropyl ether, until a white precipitate was obtained with melting point 92°C–93°C.

Tris-(3-methoxypropyl) phosphine was obtained from Mallinckrodt, Inc. (St. Louis, MO). It was stored in ethanol solution in its chloride form, at temperatures below −10°C. The ^{99m}Tc-Q4 complex was synthesized from 3-ethoxycarbonyl-9-methyl-5,8-diazadodeca-3,9-diene-2,11-dione, tris-(3-methoxypropyl) phosphine and $^{99m}TcO_4^-$, using the labeling procedure for ^{99m}Tc-Q3 described previously (*5*), except that the temperature was lowered from 78°C to 48°C to prevent hydrolysis of the ester bond.

Myocardial Perfusion Protocol

After instrumentation, baseline blood pressure measurements were made with fluid-filled catheters attached to transducers that were calibrated against a mercury manometer. Left atrial pressure, systemic arterial pressure and ECG lead II were continuously recorded on a polygraph (model 7D; Grass Instruments). The LCX (^{99m}Tc-Q3, n = 6 dogs; ^{99m}Tc-Q12, n = 4 dogs) or LAD (all remaining animals) was ligated, and the animal was allowed to stabilize for 15 min. Visible evidence of myocardial ischemia (e.g., epicardial cyanosis) was present in the distribution of the occluded artery in each animal. ST-segment shifts that were consistent with myocardial ischemia were also present on the ECG after coronary ligation. Dipyridamole was then infused at a constant rate over 4 min. Four dogs received 0.32 mg/kg (^{99m}Tc-Q3, n = 2 dogs; ^{99m}Tc-Q12, n = 2 dogs) of dipyridamole, and one dog was given 0.84 mg/kg (^{99m}Tc-Q3). The remaining animals received a standard dose of 0.56 mg/kg. Hemodynamic measurements were again obtained. Four minutes after the completion of the infusion, 10.0 mCi of the selected technetium tracer were injected intravenously. In five dogs (^{99m}Tc-sestamibi, n = 3; ^{99m}Tc-Q4, n = 2), 1.0 mCi of ^{201}Tl was coinjected with the selected technetium compound.

Regional MBF was determined with radiolabeled microspheres by the method of Heymann et al. (*25*). Microspheres were injected 1 min after the tracer injection. Blood was withdrawn from the ascending aorta at a constant rate (Harvard Apparatus) into a heparinized syringe over 3 min. Blood withdrawal was initiated 15 sec before 1 million–3 million 15-μm spheres, labeled with ^{51}Cr, ^{103}Ru, ^{95}Nb or ^{141}Ce, were rapidly injected into the left atrium. The number of injected microspheres was estimated to yield 350-1000 microspheres/g and 100 mg/kg of normally perfused myocardium. The heart rate and systemic blood pressure remained constant during a mean interval of 7 min after the injection of the tracer(s). Each dog was then killed with intravenous pentobarbital (100 mg/kg body weight), and the heart was removed from the chest. The right ventricular free wall and atria were removed. The left ventricle and septum were sliced into four adjacent rings from apex to base. The area of myocardium served by the nonligated coronary artery was demarcated to obtain samples (mean, n = 17 ± 2) that were representative of "normal" nonischemic myocardium. The myocardium was subsequently sliced into transmural samples. The samples were weighed and placed in counting vials, along with 10% formalin. Mean sample weight was 1.2 g, with a range of 0.47 g–2.18 g. About 70 samples were obtained for each experiment. Within 4 hr after the animal was killed, each sample was counted for ^{99m}Tc activity (window = 110 keV–150 keV) in a gamma well counter with a multichannel analyzer (COBRA II; Packard Instrument Co., Meriden, CT). The samples from each animal coinjected with ^{201}Tl and ^{99m}Tc were counted using appropriate energy windows for ^{201}Tl (60 keV–92 keV) and ^{99m}Tc (110 keV–150 keV). After allowing >10 half-lives for decay of ^{99m}Tc, the samples were recounted for ^{201}Tl activity. The spillover of ^{201}Tl activity into the ^{99m}Tc window was determined for each experiment and subtracted from ^{99m}Tc activity after correction for radioactivity decay. Microsphere reference blood sample activity was obtained for the appropriate windows for ^{141}Ce (120 keV–200 keV), ^{51}Cr (270 keV–370 keV), ^{103}Ru (440 keV–550 keV) or ^{95}Nb (700 keV–815 keV), after perfusion tracer activity was allowed to decay to background levels.

MBF in ml/min/g were calculated from the ratio of myocardial microsphere counts per gram of myocardium (Mc) times the rate of arterial blood withdrawal into a syringe (SBF, in ml/min), divided by total microsphere counts in the reference blood sample (Bc):

$$MBF = Mc \times SBF/Bc.$$

Data Analysis

Data are expressed as the mean ± s.e. A p value of <0.05 was considered significant. Significant changes in hemodynamic parameters within an individual tracer group were assessed by a two-tailed paired Student's t-test. The significance of a difference in means between tracer groups was assessed using a multivariate general linear hypothesis procedure with a one-way analysis of variance design. To combine data from different animals for a given tracer, the microsphere determined MBF (ml/min/g) and myocardial activity (counts/g) from each tissue sample were normalized by three previously reported methods (*7,8,21*). First,

TABLE 1
Hemodynamics (mean ± s.e.) during Baseline, Post-Coronary Artery Ligation and during Pharmacologic Stress Induced with Dipyridamole

Hemodynamic parameter	Radioperfusion tracer						
	^{201}Tl, n = 5 (5)	^{99m}Tc-Q3, n = 9 (8)	^{99m}Tc-Q4, n = 4 (3)	^{99m}Tc-Q12, n = 7 (7)	^{99m}Tc-tetrofosmin, n = 4 (3)	^{99m}Tc-sestamibi, n = 4 (4)	^{99m}TcN-NOET, n = 4 (4)
Heart rate (bpm)							
Baseline	125 ± 8	111 ± 9	142 ± 20	118 ± 7	115 ± 10	119 ± 9	119 ± 4
Ligation	113 ± 9	119 ± 7	125 ± 6	110 ± 10	115 ± 3	110 ± 11	116 ± 8
Dipyridamole	117 ± 13	124 ± 8	118± 14	123 ± 10	119 ± 10	121 ± 16	115 ± 12
Systolic blood pressure (mmHg)							
Baseline	141 ± 11	136 ± 6	150 ± 18	141 ± 10	140 ± 8	130 ± 4	160 ± 6
Ligation	118 ± 16	119 ± 6	145 ± 13	118 ± 11*	127 ± 7	105 ± 13	147 ± 3*
Dipyridamole	98 ± 5*	100 ± 8*	110 ± 2	110 ± 11*	101 ± 21*	94 ± 5*	120 ± 11*
Diastolic blood pressure (mmHg)							
Baseline	107 ± 9	96 ± 4	117 ± 9	103 ± 6	102 ± 6	100 ± 7	111 ± 7
Ligation	95 ± 13	93 ± 5	116 ± 10	88 ± 8*	92 ± 10	85 ± 11	109 ± 8
Dipyridamole	70 ± 3*	65 ± 5*	82 ± 4	76 ± 8*†	63 ± 19	69 ± 3*	82 ± 9*
Left atrial pressure (mmHg)							
Baseline	10 ± 2	10 ± 1	9 ± 2	9 ± 1	10 ± 2	9 ± 3	13 ± 2
Ligation	14 ± 3*	16 ± 2*	13 ± 5	12 ± 1*	13 ± 3	13 ± 3	20 ± 3
Dipyridamole	13 ± 3*	13 ± 1*	12 ± 4	11 ± 1	11 ± 3	12 ± 3*	18 ± 3

*$p < 0.05$ versus baseline.
†$p < 0.05$ versus ligation.
Numbers in parentheses indicate number in each group with hemodynamic observations available.

the calculated myocardial activity and MBF for each sample were normalized to the mean tracer activity and MBF from each individual dog (*21*). Second, the myocardial activity and MBF for each sample were expressed as a percentage of the mean activity and MBF from the normal, nonischemic zone from each individual animal (*7*). Third, the myocardial activity and MBF for each sample were normalized to the maximum activity and maximum microsphere determined MBF from each individual animal (*8*). In the animals with LAD occlusion, the base of the posterior-lateral free wall represented the normal, nonischemic zone of myocardium. In animals with LCX occlusion, the anteroseptal wall represented the normal, nonischemic zone. The paired data (tracer activity versus MBF) were plotted and analyzed by linear regression and the corresponding correlation coefficient, best-fit line slope and y-intercept were obtained. The differences in regression lines were determined using an analysis of variance for differences between slopes and between intercepts. Data were recalculated after exclusion of five animals that received a dose of dipyridamole other than 0.56 mg/kg. No significant differences in uptake characteristics were observed for these animals, and their data were included in the final calculation.

RESULTS

Hemodynamic Analysis

Hemodynamic parameters were obtained at baseline, 15 min after coronary artery occlusion (postocclusion) and at the time of tracer and microsphere administration (postdipyridamole). Complete hemodynamic data were available for 29 of 32 dogs. Mean hemodynamic data for individual tracer groups are presented in Table 1. After dipyridamole administration, each group showed a statistically significant decrease (mean, 33.0 mmHg ± 4 mmHg) in systolic blood pressure from baseline, except for the ^{99m}Tc-Q4 group, which showed a nonsignificant downward trend. A significant decrease in diastolic blood pressure (mean, 32.0 mmHg ± 4.0 mmHg) from baseline measurements was also noted in all groups, except in the ^{99m}Tc-Q4 and ^{99m}Tc-tetrofosmin groups, which displayed a downward trend only. At the time of tracer administration, the ^{201}Tl, ^{99m}Tc-Q3 and ^{99m}Tc-sestamibi groups all had significant elevations in left atrial pressure (mean increase, 4.0 mmHg ± 1.0 mmHg) compared to baseline measurements. The lack of statistically significant hemodynamic changes (i.e., biologic response to dipyridamole) within other groups must be viewed cautiously, due to the less-than-desired power of 0.80 found in these analyses. No significant changes in heart rate were noted in individual groups among the baseline, postocclusion and postdipyridamole measurements. When between-group comparisons of the mean baseline, postocclusion and postdipyridamole hemodynamics were made, no significant differences were present.

Myocardial Extraction Versus Myocardial Blood Flow of Radioperfusion Tracers

Disproportionately low tracer activity in high-blood-flow (so-called "roll-off") myocardial samples was evident for each tracer group when data were plotted without normalization, although the flow value at which this roll-off of tracer activity occurred was variable among tracers. Single experiment plots of tissue sample tracer activity versus MBF (Fig. 1) for ^{99m}Tc-Q3 and ^{99m}Tc-sestamibi illustrate the effects of normalization (by average, normal and maximum) on the shape of the activity versus MBF relationship. Experiments with similar maximum MBF were chosen for comparison. In general, each normalization method tended to underestimate the intercept, overestimate the slope and obscure the tissue sample tracer activity roll-off at high flows.

The tracer group scatter plots relating myocardial uptake to myocardial MBF for all experimental data are shown using

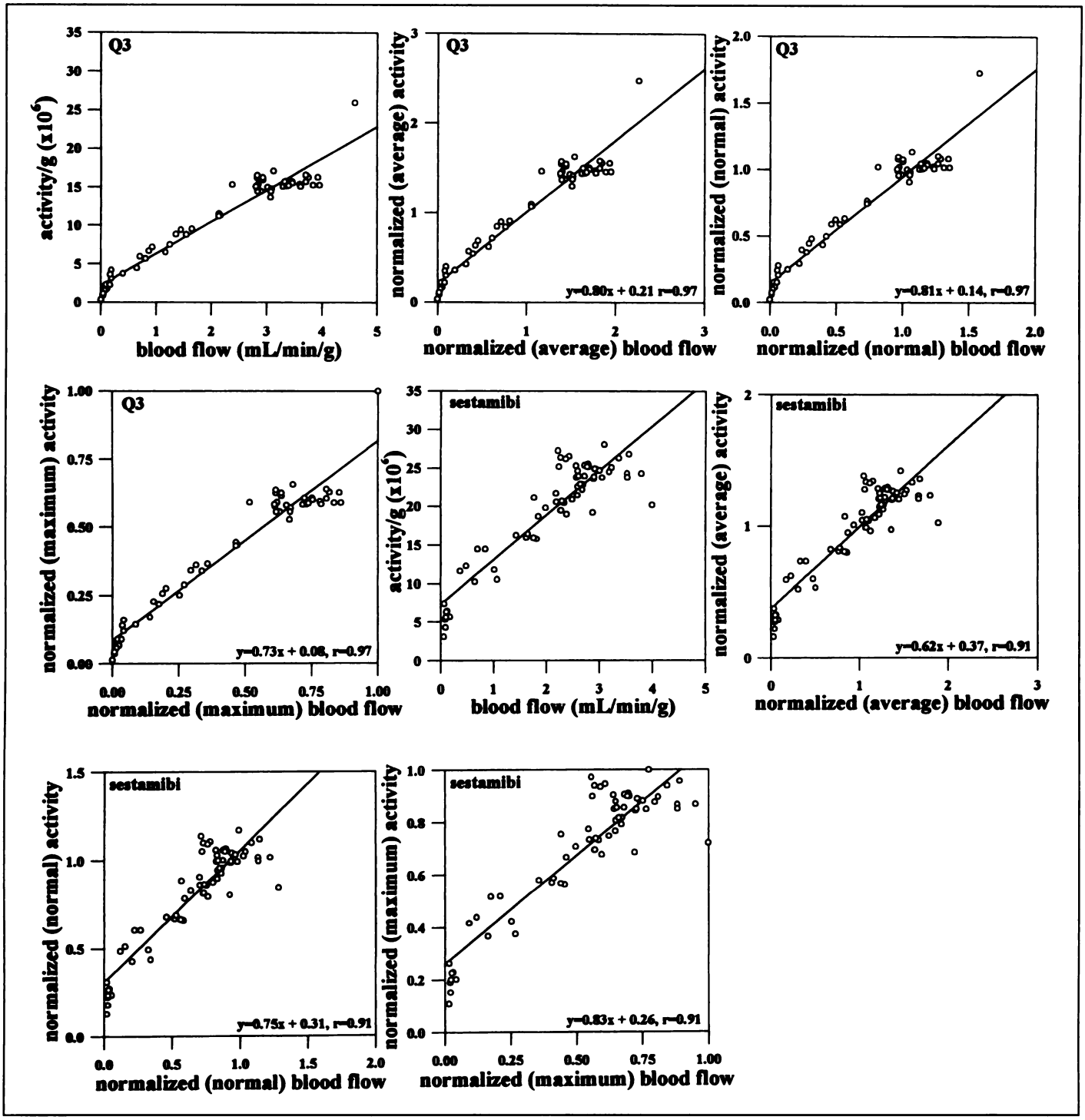

FIGURE 1. Representative ^{99m}Tc-Q3 and ^{99m}Tc-sestamibi plots of myocardial tracer activity versus MBF before normalization and after analysis by average, normal and maximum normalization methods.

three separate normalization methods (Fig. 2, average; Fig. 3, normal; Fig. 4, maximum). The range of MBF obtained for each tracer group, the linear regression analysis and a comparison between other tracer slopes and intercepts are included with each scatter plot. There was a statistically significant linear relationship ($p < 0.0001$) between the normalized myocardial activity and the normalized microsphere-determined MBF for each of the tracers. The correlation coefficient remained relatively constant regardless of the normalization technique used. In contrast, the slope and y-intercept for a given tracer depended on the normalization technique used. As a higher denominator was used for normalization, the best-fit line slope and y-intercept tended to shift toward an optimal slope of 1.0 and an intercept at the origin. Thus, the data normalized to the maximum myocardial activity and MBF displayed the most ideal slope and intercepts among the three normalization techniques used.

When linear regression analyses of tracers were compared, some statistical differences were appreciated between individual slopes and y-intercepts, despite small differences in absolute numbers. This result is, in part, due to the large number of myocardial samples acquired for each tracer group. The slope and y-intercept for ^{201}Tl were significantly more ideal (i.e., close to 1.0 and 0.0, respectively) than were these values for all

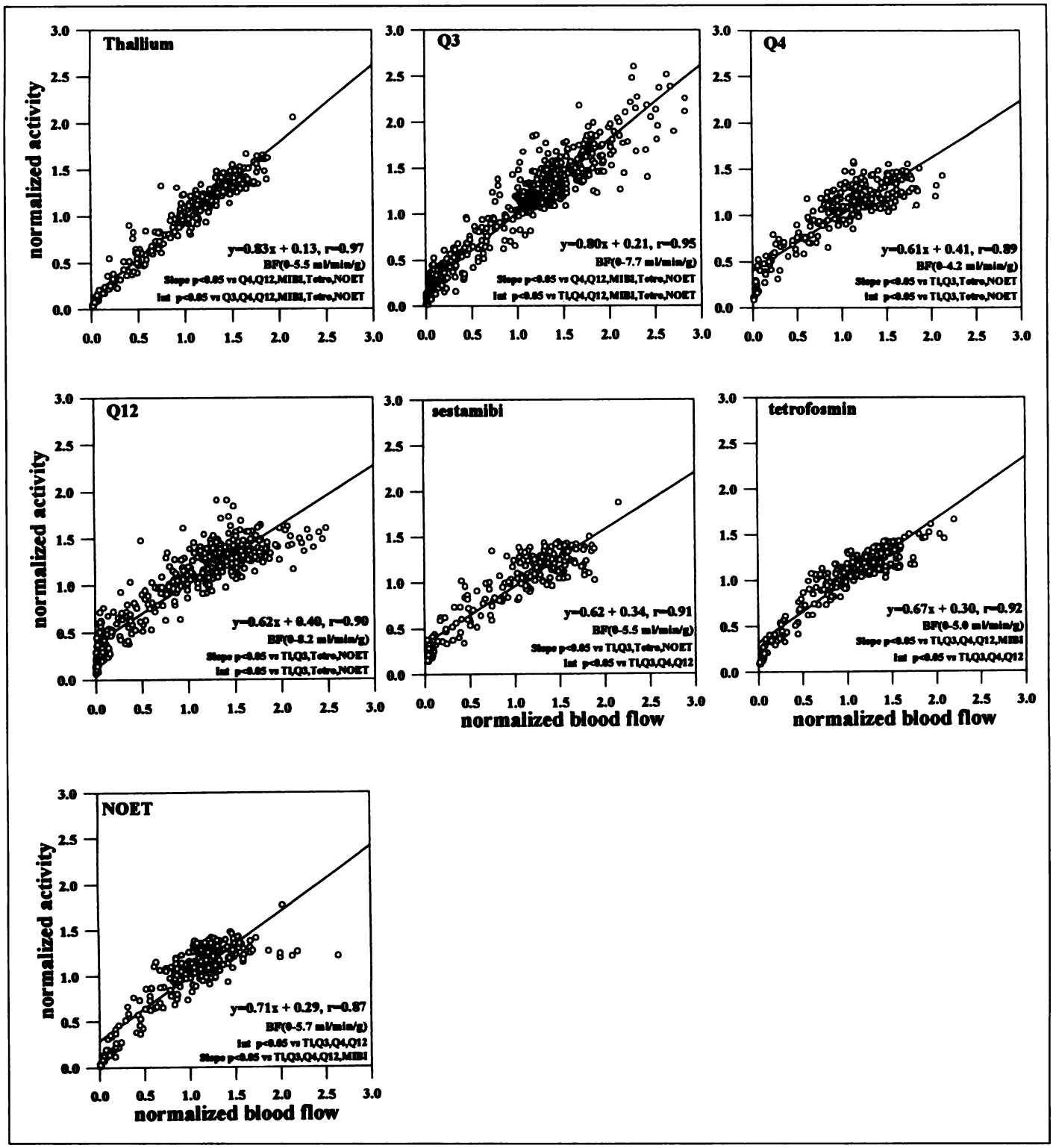

FIGURE 2. Aggregate study group data of normalized average myocardial tracer activity versus normalized average MBF for each of seven tracers. BF = blood flow; Int = intercept.

other tracers ($p < 0.001$). Likewise, the slope and y-intercept for ^{99m}Tc-Q3 were significantly closer to ideal than were the values for the other technetium tracers ($p < 0.001$), regardless of the normalization method used. Differences among the other technetium tracers were dependent on the normalization method used.

The percentage of the total number of MBF values in a tracer group that fall in the central ischemic and normal zones are listed in Table 2. To try to compensate for differences in the distribution of MBF between tracer groups, the non-normalized tissue tracer activity per gram and MBF were averaged into 0.2-ml/min/g "bins," and then the binned data were normalized by the average tracer activity and MBF (Fig. 5). By this technique, statistically significant differences between ^{99m}Tc-Q3 and the remaining ^{99m}Tc-based agents were lost, but the overall trends were maintained.

DISCUSSION

Thallium-201 remains the cornerstone of myocardial perfusion imaging, despite the introduction of new technetium-

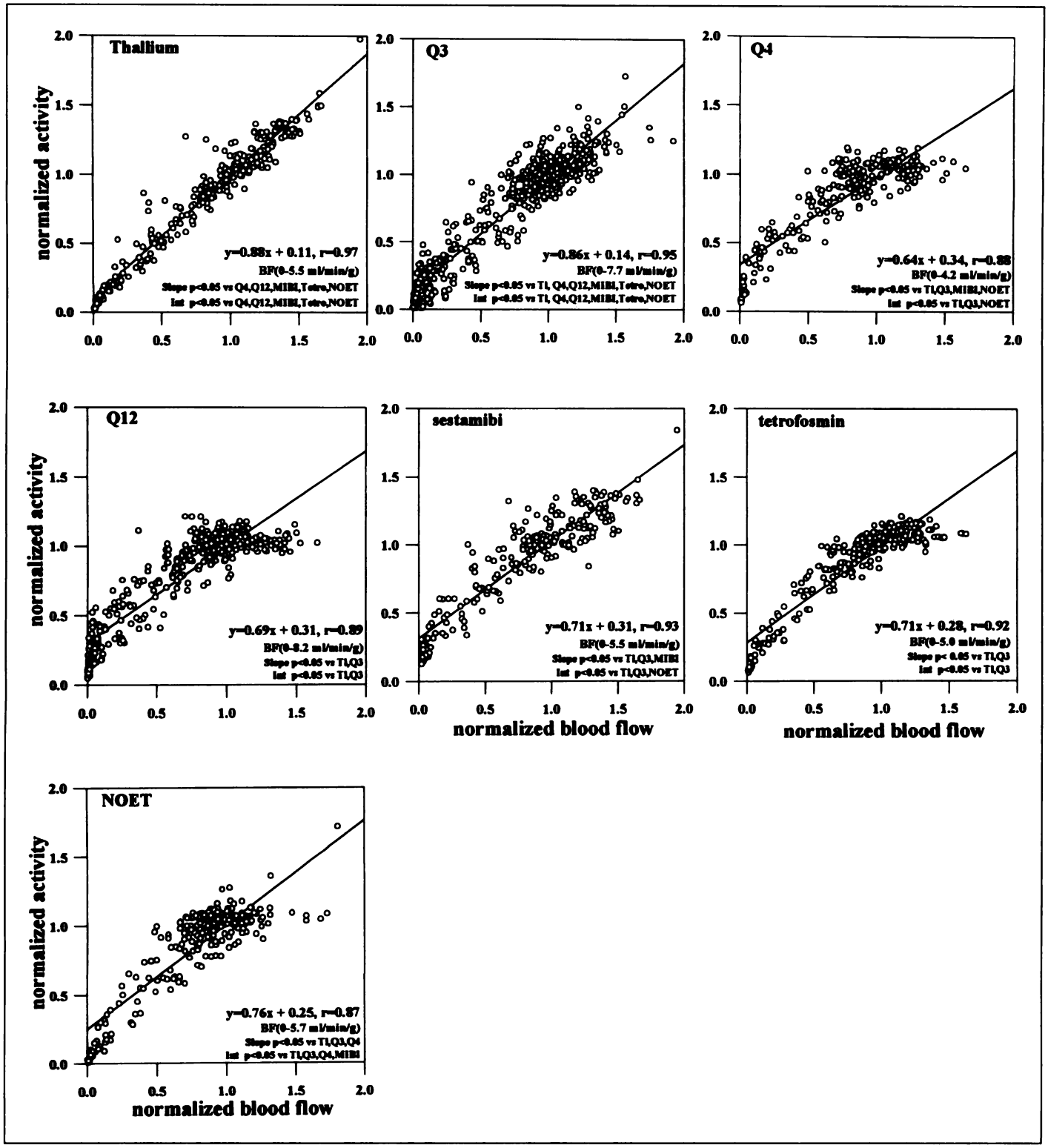

FIGURE 3. Aggregate study group data of normalized normal (nonischemic) myocardial tracer activity versus normalized normal (nonischemic) MBF for each of seven tracers. BF = blood flow; Int = intercept.

labeled compounds. There are two main reasons for this. First, no other radioperfusion agent to date has equaled the myocardial extraction and flow kinetics of ^{201}Tl. Second, the myocardial redistribution properties of ^{201}Tl after initial uptake offer a relatively inexpensive and readily available means of assessing myocardial viability that is unmatched by any other nuclear imaging modality. Regardless of these favorable attributes, the limiting physical properties of ^{201}Tl (e.g., soft tissue attenuation, long physical half life and low energy) continue to fuel the need for the development of new myocardial tracers.

We present a direct comparison of the myocardial uptake kinetics of seven perfusion tracers (^{201}Tl, ^{99m}Tc-Q3, ^{99m}Tc-Q4, ^{99m}Tc-Q12, ^{99m}Tc-sestamibi, ^{99m}Tc-tetrofosmin and ^{99m}Tc-N-NOET) and report initial uptake characteristics of ^{99m}Tc-Q4 in

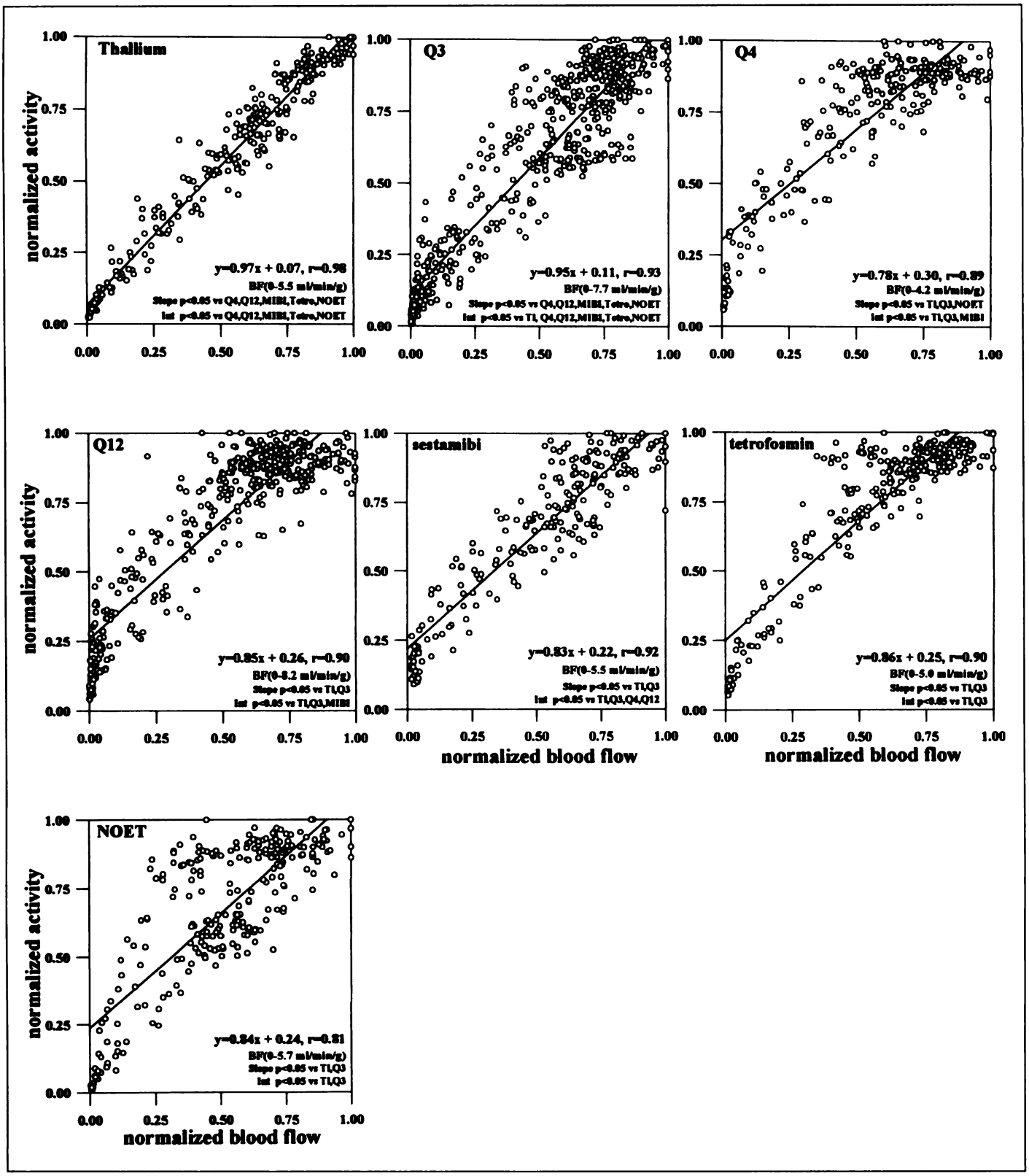

FIGURE 4.. Aggregate study group data of normalized maximal myocardial tracer activity versus normalized maximal MBF for each of seven tracers. BF = blood flow; Int = intercept.

a canine model of myocardial ischemia. To combine data from different experiments for comparison with previous investigations, the data from each experiment were normalized.

The best method for normalizing these data remains unclear. Many early tracer studies either presented non-normalized data or reported the myocardial activity (and usually MBF) as a percentage of the nonischemic myocardium, with some variation in methodology (*12,14,15*). The latter normalization approach appears reasonable because relating the MBF and tracer activity in the ischemic region to a region of remote nonischemic myocardium, in theory, is analogous to the interpretation of nuclear perfusion images. However, in several recent radiotracer studies (*5,6,12*), the myocardial tracer activity and MBF of each myocardial sample were normalized to the average

TABLE 2
Percentage of Total Number of Myocardial Samples That Fall within the Central Ischemic (0 ml/min/g–0.4 ml/min/g) and Normal (>0.4 ml/min/g) Blood Flow Regions

Flow	Radioperfusion tracer						
	^{201}Tl	^{99m}Tc-Q3	^{99m}Tc-Q4	^{99m}Tc-Q12	^{99m}Tc-sestamibi	^{99m}Tc-tetrofosmin	^{99m}TcN-NOET
Ischemic	20.6	25.7	15.1	23.6	18.9	10.4	13.0
Normal	79.4	74.3	84.9	76.4	81.1	89.6	87.0

activity per unit mass of the entire ventricle and the average MBF, respectively (*21*). Yet, another normalization method uses percentages of maximum myocardial tracer activity and MBF (*8*). We do not discuss the theoretical validity of these three normalization techniques. However, by applying each normalization method to our datasets, we were able to assess their effects on the characteristic flow-uptake relationship for each tracer.

Myocardial uptake of each tracer correlated well with MBF early after a coronary occlusion, but important differences were observed. Thallium-201 uptake displayed a more linear relationship to MBF flow, with a slope approaching unity and a y-intercept near zero, than that observed for each of the ^{99m}Tc-based tracers. However, ^{99m}Tc-Q3 appeared to have a slope and y-intercept closer to ideal than did the other ^{99m}Tc-based tracers. The favorable early myocardial uptake kinetics of ^{201}Tl in this study are consistent with previous investigations, despite variations in methodology (*9–11,13–17*). Previous reported methods applied to analyze myocardial kinetics of ^{99m}Tc-sestamibi also differ (*7,16,18,20*). Available data for comparison of the remaining tracers are very limited (*8,12*).

An observation of the results presented here is that data that are normalized by maximal activity and MBF are more susceptible to error if a single large outlying maximum value is present in the dataset. Normalization of a dataset with an extreme value will tend to bring the y-intercept closer to zero and will have a disproportionate effect on the tracer uptake versus MBF curve. An example of this is seen in the ^{99m}Tc-Q3 plot in Figure 1, in which a single sample represents the largest MBF and tracer activity values. Although elimination of this value from the analysis had little effect on the slope and intercept of the average or normal (nonischemic) normalization curves, the slope of the maximum normalization curve increased from 0.73 to 0.96. Consistently, normalizing by maximal myocardial tracer activity and MBF resulted in a higher slope and lower intercept than did normalizing by average or normal nonischemic values (Figs. 2–4).

Subsets of our ^{99m}Tc-Q3 and ^{99m}Tc-Q12 data have been published previously (*5,6*). The ^{99m}Tc-Q12 myocardial activity expressed as a percentage of average was related to non-normalized MBF over a MBF range of 0 ml/min/g–2.0 ml/min/g by the relationship $y = 0.64x + 0.35$ ($r = 0.88$). There was a plateau of myocardial tracer extraction above a flow of 2.0 ml/min/g, so these data points were not included in the previous (*6*) linear regression analysis. Here, both axes (myocardial activity and MBF) were expressed as a percentage of average, revealing a more linear relationship over the entire MBF range. Therefore, all the data points were included in the linear regression analysis.

Why the myocardial uptake kinetics of the cationic tracer ^{99m}Tc-Q3 may be more similar to the early-uptake kinetics of ^{201}Tl and less similar to the other radiolabeled perfusion agents in our model is unclear. One may speculate that the observed early myocardial uptake for ^{99m}Tc-Q3 may be due, in part, to its compact and balanced structure (*5*). Previous studies have suggested that ^{99m}Tc-Q3 exhibits more rapid hepatic clearance than does ^{99m}Tc-sestamibi (*26*) and a lower background lung activity than do ^{99m}Tc-Q12 and ^{99m}TcN-NOET, not long after administration (*27–29*). In addition, the myocardial retention of ^{99m}Tc-Q3 at 1.5 hr after injection is comparable to that of ^{99m}Tc-sestamibi and ^{99m}Tc-tetrofosmin 1 hr after injection but significantly lower than that reported for ^{99m}Tc-Q12 (*27,30*).

There are several limitations of our study, such as the absence of ^{99m}Tc-teboroxime. A valid comparison of ^{99m}Tc-teboroxime uptake would not be possible here, as substantial myocardial washout of teboroxime would be expected between the time of tracer injection and the time of tissue sampling 7 min later. We also deviated from the standard dipyridamole dosage of 0.56 mg/kg in two of the tracers groups studied. However, no correlation between dipyridamole dose and maximal MBF or linear regression parameters was noted. The initial tracer distribution of each of the tracers studied may depend on the distribution of MBF, specifically, the extent of myocardial ischemia and pharmacologically induced hyperemia. Although the data subjected to linear regression were normally distributed for each tracer group, we attempted to force the MBF distribution among tracer groups to be evenly distributed by binning the data. The results from this analysis are consistent with the conclusion that ^{99m}Tc-Q3 initial uptake is closer to ideal than the remaining ^{99m}Tc tracer studied. Finally, our findings must be viewed in the context of an open-chest anesthetized canine model using direct myocardial counts only, of which other factors that are important in clinical imaging, such as soft tissue attenuation and dosimetry of other organs, are not considered.

Clinical Implications

The assumption of a linear relationship between myocardial extraction and MBF is the foundation upon which radionuclide myocardial tracers are used in diagnostic clinical perfusion imaging. The radiotracer with the uptake that is most closely related to MBF (i.e., myocardial tracer extraction parallels MBF) would be expected to lend a greater diagnostic sensitivity in detecting mild-to-moderate coronary artery stenoses using nuclear perfusion imaging (*31*). If this principle holds true and all other imaging properties of the tracer are equal, then the results of the present investigation support an increased diagnostic sensitivity of ^{201}Tl and, possibly, ^{99m}Tc-Q3 to the other technetium tracers studied for detection of mild-to-moderate stenoses. However, the interpretation of results from previous clinical investigations comparing ^{201}Tl imaging with ^{99m}Tc-sestamibi, ^{99m}Tc-Q12, ^{99m}Tc-tetrofosmin or ^{99m}TcN-NOET does not concur with this conclusion. In fact, these agents have been reported to have comparable diagnostic sensitivity and specificity to ^{201}Tl (*26,29,32,33*). The reason for the disparate conclusions may be due, in part, to the more favorable flow-uptake kinetics of ^{201}Tl being offset by the better counting statistics, superior resolution and reduced attenuation of the higher-energy technetium compounds. Recent investigations, directly assessing the myocardial perfusion defect size between a ^{99m}Tc tracer and ^{201}Tl using SPECT, support our findings

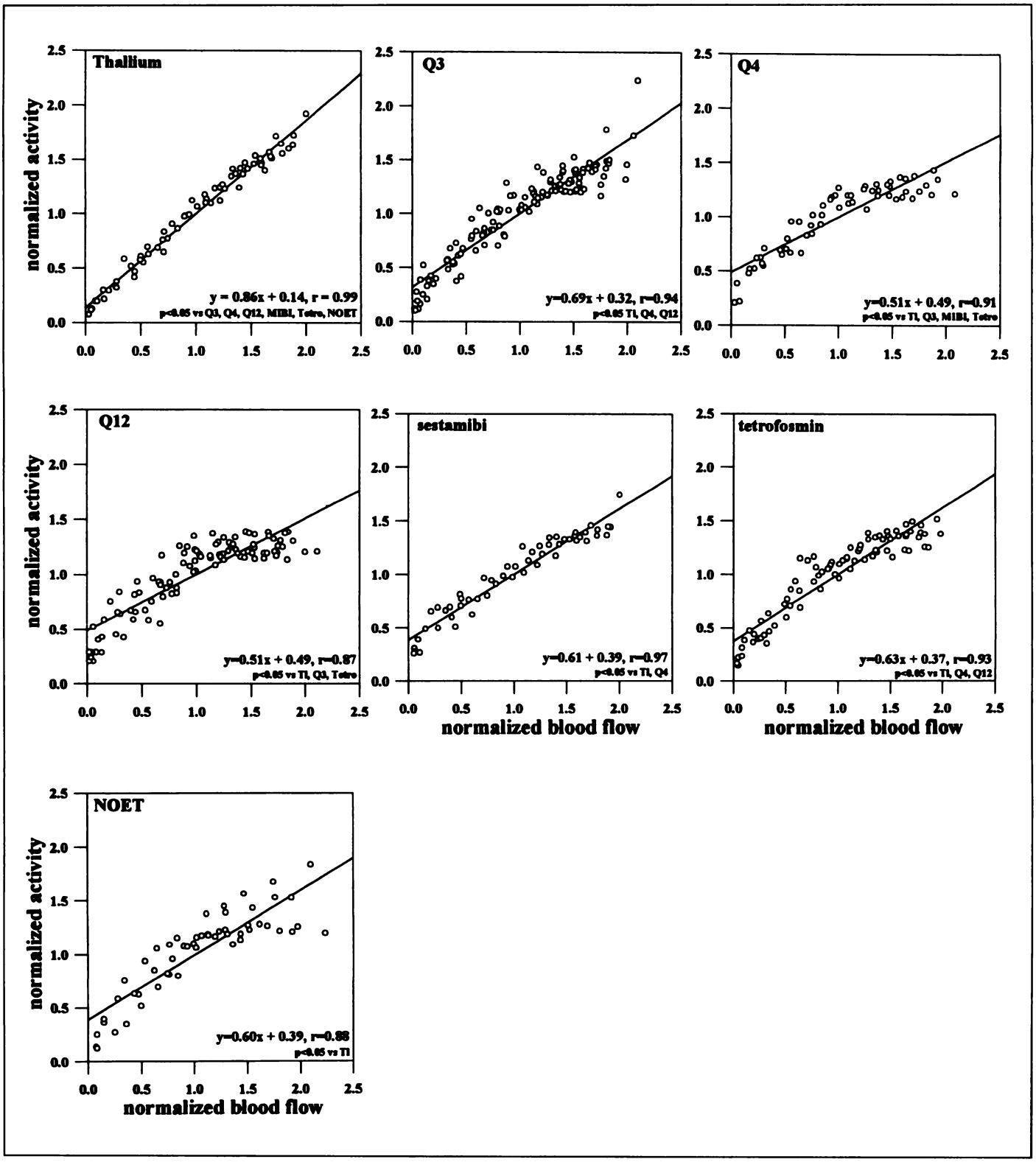

FIGURE 5. Aggregate study group data first binned into 0.2-ml/min/g bins for each experiment and then normalized by average tracer activity and MBF for each of seven tracers. BF = blood flow.

(*34–37*). These studies revealed an underestimation of the size of myocardial perfusion defects with the ^{99m}Tc tracer compared to defect size obtained with ^{201}Tl. As one might expect, the differences were mainly in the detection of mild-to-moderately severe coronary occlusions rather than in detection of severe perfusion defects that are associated with complete coronary artery occlusion.

A perfusion tracer that possesses the myocardial uptake versus MBF properties of ^{201}Tl with the higher photon energy of ^{99m}Tc might be expected to yield a diagnostic sensitivity that is better than that of ^{201}Tl at all MBFs. Thus, the potential of ^{99m}Tc-Q3 in clinical nuclear imaging is intriguing. Gerson et al. (*38*), studying 27 patients, found a nonsignificant trend toward higher sensitivity for detection of coronary artery disease with ^{99m}Tc-Q3 than they did with ^{201}Tl imaging. The future role of ^{99m}Tc-Q3 as a clinical myocardial perfusion imaging agent

remains undetermined and will only be determined if results from a multicenter study become available.

CONCLUSION

When data from multiple experiments are combined into the model presented here, data normalization should be standardized to allow for adequate comparisons of experimental results among research groups. Based on our data, normalization by maximum tracer uptake and maximum MBF may be the least appropriate because it minimizes differences among tracers by artificially increasing the slope and decreasing the intercept; the data may be biased by a single data point. Additionally, in an anesthetized open-chest canine model of regional myocardial ischemia with dipyridamole-induced hyperemia, ^{201}Tl myocardial flow kinetics are superior to those of the ^{99m}Tc-based imaging agents studied. The tissue tracer uptake versus MBF characteristics of ^{99m}Tc-Q3 appear to be promising, relative to the other technetium tracers studied, and appear to behave more similarly to ^{201}Tl than do the other ^{99m}Tc-based agents.

ACKNOWLEDGMENTS

This study was funded in part by a grant from Mallinckrodt, Inc. (St. Louis, MO). N.J.R. was supported by National Institutes of Health National Heart, Lung and Blood Institute Training Grant HL07382. We would like to thank Peter Gartside, PhD (Department of Environmental Health, Biostatistics and Epidemiology Division, University of Cincinnati), for his statistical consultation and Roberto Pasqualini, PhD (CIS Bio International, Gif-sur-Yvette, France), for the generous support of the chemical ligand and methodology necessary in preparing ^{99m}TcN-NOET. We would also like to acknowledge the excellent technical contributions of Gary Flesher and Thomas Frede.

REFERENCES

1. White CW, Wilson RF, Marcus ML. Methods of measuring myocardial blood flow in humans. *Prog Cardiovasc Dis* 1988;31:79–94.
2. West JW, Bellet S, Manzoli UC, Muller OF. Effects of persantin (RA8), a new coronary vasodilator, on coronary blood flow and cardiac dynamics in a dog. *Circ Res* 1961;10:35–44.
3. Hutchins GD, Schwaiger M, Rosenpike KC, Krivokapich J, Schelbert H, Kuhl DE. Noninvasive quantification of regional blood flow in the human heart using N-13 ammonia and dynamic positron emission tomographic imaging. *J Am Coll Cardiol* 1990;15:1032–1042.
4. Bergmann SR, Herrero P, Markham J, Weinheimer CJ, Walsh MN. Noninvasive quantification of myocardial blood flow in human subjects with oxygen-15-labeled water and positron emission tomography. *J Am Coll Cardiol* 1989;14:639–652.
5. Gerson MC, Millard RW, McGoron AJ, et al. Myocardial uptake and kinetic properties of technetium-99m-Q3 in dogs. *J Nucl Med* 1994;35:1698–1706.
6. Gerson MC, Millard RW, Roszell NJ, et al. Kinetic properties of technetium-99m-Q12 in canine myocardium. *Circulation* 1994;89:1291–1213.
7. Glover KF, Okada RD. Myocardial kinetics of Tc-MIBI in canine myocardium after dipyridamole. *Circulation* 1990;81:628–636.
8. Ghezzi C, Fagret D, Arvieux CC, et al. Myocardial kinetics of TcN-NOET: a neutral lipophilic complex tracer of regional myocardial blood flow. *J Nucl Med* 1995;36: 1069–1077.
9. Pohost GM, Zir LM, Moore RH, McKusick KA, Guiney TE, Beller GA. Differentiation of transiently ischemic from infarcted myocardium by serial imaging after a single dose of thallium-201. *Circulation* 1977;55:294–302.
10. Mueller TM, Melvin ML, Ehrhardt JC, Chaudhuri, Abboud FM. Limitations of thallium-201 myocardial perfusion scintigrams. *Circulation* 1976;57:640–646.
11. Melin JA, Becker LC, Bulkley BH. Differences in thallium-201 uptake in reperfused and nonreperfused myocardial infarction. *Circ Res* 1983;53:414–419.
12. Sinusas AJ, Shi QX, Saltzberg MT, et al. Technetium-99m-tetrofosmin to assess myocardial blood flow: experimental validation in an intact canine model of ischemia. *J Nucl Med* 1994;35:664–671.
13. Strauss HW, Harrison K, Langan JK, Lebowitz E, Pitt B. Thallium-201 for myocardial imaging. Relation of thallium-201 to regional myocardial perfusion. *Circulation* 1975:641–645.
14. Nielson AB, Morris KG, Murdock R, Bruno FP, Cobb FR. Linear relationship between the distribution of thallium-201 and blood flow in ischemic and non-ischemic myocardium during exercise. *Circulation* 1980;61:797–801.
15. Mays AE Jr, Cobb FR. Relationship between regional myocardial blood flow and thallium-201 distribution in the presence of coronary artery stenosis and dipyridamole-induced vasodilation. *J Clin Invest* 1984;73:1359–1366.
16. Mousa SA, Cooney JM. Detection sensitivity of coronary artery stenosis by Tc-99m-sestamibi and Tl-201 in canine models of partial and subcritical stenosis. *Cardiology* 1991;79:135–145.
17. Melon PG, Beanlands RS, DeGrado TR, Nguyen N, Petry NA, Schwaiger M. Comparison of technetium-99m sestamibi and thallium-201 retention characteristics in canine myocardium. *J Am Coll Cardiol* 1992;20:1277–1283.
18. Okada RD, Glover D, Gaffney T, Williams S. Myocardial kinetics of technetium-99m-hexakis-2-methoxy-2-methylpropyl isonitrile. *Circulation* 1988;77:491–498.
19. Mehri A, Arsenaut A, Latour J. Time course of technetium-99m sestamibi myocardial distribution in dogs with a permanent or transient coronary occlusion. *Eur J Nucl Med* 1994;21:481–487.
20. Glover DK, Ruiz M, Edwards NC, et al. Comparison between thallium-201 and Tc-99m-sestamibi uptake during adenosine-induced vasodilation as a function of coronary stenosis severity. *Circulation* 1995;91:813–820.
21. Bassingthwaighte JB, Malone MA, Moffett TC, et al. Validity of microspheres deposition for regional myocardial flows. *Am J Physiol* 1987;253:H184–H193.
22. De Rosch MA, Brodack JW, Grummon GD, et al. Kit development for the ^{99m}Tc myocardial imaging agent (TechneCard^{TM}) [Abstract]. *J Nucl Med* 1992;33(suppl): 850.
23. Kwiatkowski E, Kwiatkowski M, Olechnowicz A. Metal complexes with unsymmetrical tetradentate ketoenamines derived from β-diketones or ethoxymethylene-β-dicarbonyl compounds and 1-amino-4-methyl-3-azahept-4-ene-6-one. *Inorg Chim Acta* 1984;90:145–152.
24. Claisen L. Untersuchungen uber die oxymethylenverbindungen. *Ann Chem* 1987;297: 1–69.
25. Heymann MA, Payne BD, Hoffman JE, Rudolph AM. Blood flow measurements with radionuclide-labeled particles. *Prog Cardiovasc Dis* 1977;20:55–79.
26. Wackers FJTh, Berman D, Maddahi J, et al. Technetium-99m hexakis 2-methoxy-isobutyl isonitrile: human biodistribution, dosimetry, safety and preliminary comparison to thallium-201 for myocardial perfusion imaging. *J Nucl Med* 1989;30:301–311.
27. Rossetti C, Vanoli G, Paganelli G, et al. Human biodistribution, dosimetry and clinical us of technetium(III)-99m-Q12. *J Nucl Med* 1994;35:1571–1580.
28. Gerson MC, Lukes J, Deutsch E, et al. Comparison of technetium 99m Q12 and thallium 201 for detection of angiographically documented coronary artery disease in humans. *J Nucl Cardiol* 1994;1:499–508.
29. Fagret D, Marie PY, Brunotte F, et al. Myocardial perfusion imaging with technetium-99m-Tc NOET: comparison with thallium-201 and coronary angiography. *J Nucl Med* 1995;36:936–943.
30. Rohe RC, Thomas SR, Stabin MG, et al. Biokinetics and dosimetry in healthy volunteers for two-injection (rest–stress) protocol of the myocardial perfusion imaging agent technetium 99m-labeled Q3. *J Nucl Cardiol* 1995:395–404.
31. Gould KL. Noninvasive assessment of coronary stenoses by myocardial perfusion imaging during pharmacologic coronary vasodilation. *Am J Cardiol* 1978;41:267–278.
32. Hendel RC, Gerson MC, Verani MS, et al. Perfusion imaging with Tc-99m furifosmin (Q12): multicenter phase III trial to evaluate safety and comparative efficacy [Abstract]. *Circulation* 1994;90(suppl I):I-449.
33. Zaret BL, Rigo P, Wackers FJT, et al. Myocardial perfusion imaging with Tc99m tetrofosmin: comparison to Tl-201 imaging and coronary angiography in a Phase III multicenter trial. *Circulation* 1995;91:313–319.
34. Leon AR, Eisner RL, Martin SE, et al. Comparison of single-photon emission computed tomographic (SPECT) myocardial perfusion imaging with thallium-201 and technetium-99m sestamibi in dogs. *J Am Coll Cardiol* 1992;20:1612–1625.
35. Narahara KA, Vilanueva-Meyer J, Thompson CJ, Brizendine M, Mena I. Comparison of thallium-201 and technetium-99m hexakis 2-methoxyisobutyl isonitrile single-photon emission computed tomography for estimating the extent of myocardial ischemia and infarction in coronary artery disease. *Am J Cardiol* 1990;66:1438–1444.
36. Maublant JC, Marcaggi X, Lusson J, et al. Comparison between thallium-201 and technetium-99m methoxyisobutyl isonitrile defect size in single-photon emission computed tomography at rest, exercise and redistribution in coronary artery disease. *Am J Cardiol* 1992;69:183–187.
37. Matsunari I, Fujino S, Taki J, et al. Comparison of defect size between thallium-201 and technetium-99m tetrofosmin myocardial single-photon emission computed tomography in patients with single-vessel coronary artery disease. *Am J Cardiol* 1996;77: 350–354.
38. Gerson MC, Lukes J, Deutsch E, et al. Comparison of technetium-99m-Q3 and thallium-201 for detection of coronary artery disease in humans. *J Nucl Med* 1994;35:580–586.